Clinical log data analysis for assessing the accuracy of the CyberKnife fiducial-free lung tumor tracking system

Nakayama, Masao ; Nishimura, Hideki ; Mayahara, Hiroshi ; Nakamura, Masaki ; Uehara, Kazuyuki ; Tsudou, Shinji ; Harada, Aya ; Akasaka,…

(Citation)
Practical Radiation Oncology,8(2):e63-e70

(Issue Date)
2018

(Resource Type)
journal article

(Version)
Accepted Manuscript

Clinical log data analysis for assessing the accuracy of the CyberKnife fiducial-free lung tumor tracking system

Masao Nakayama PhD[1, 2], Hideki Nishimura MD, PhD[1], Hiroshi Mayahara MD, PhD [1], Masaki Nakamura MD[1], Kazuyuki Uehara PhD[1], Shinji Tsudou MSc[1], Aya Harada MD, PhD [1], Hiroaki Akasaka PhD[2], Ryohei Sasaki MD, PhD [2]

[1] Division of Radiation Oncology, Kobe Minimally Invasive Cancer Center, 8-5-1 Minatojima-nakamachi, Chuou-ku, Kobe City, Hyogo 650-0046, Japan
[2] Division of Radiation Oncology, Kobe University Graduate School of Medicine, 7-5-2 Kusunokicho, Chuou-ku, Kobe City, Hyogo, 650-0017, Japan

Corresponding author:
Masao Nakayama, Ph.D.
Division of Radiation Oncology, Kobe Minimally Invasive Cancer Center, 8-5-1 Minatojima-nakamachi, Chuou-ku, Kobe City, Hyogo 650-0046, Japan
Tel: +81-78-3044100, Fax: +81-78-3040041
E-mail: naka2008@med.kobe-u.ac.jp

Running title: CyberKnife lung tumor tracking accuracy

Acknowledgement:
This work was partially supported by JSPS KAKENHI Grant Number 16K10395.

Conflicts of Interest Notification
The authors declare that they have no conflicts of interest.

Abstract

Purpose: The CyberKnife Xsight Lung Tracking (XLT) and 1-View tracking systems can synchronize beam targeting to a visible lung tumor with respiratory motion during irradiation without requiring internal fiducial markers. The systems utilize a correlation model that relates external marker positions to tumor positions as well as a prediction model that predicts the target's future position. In this study, the correlation and prediction model uncertainties related to the CyberKnife fiducial-free tumor tracking system were evaluated using clinical log data.

Methods and materials: Data from 211 fractions in 42 patients with lung tumors were analyzed. Log files produced by the CyberKnife Synchrony system were acquired after each treatment; the mean correlation and prediction errors for each patient were calculated. Additionally, we examined the tracking tumor-related parameters and analyzed the relationships between the model errors and tracking tumor-related parameters.

Results: The overall means ± standard deviations (SDs) of the correlation errors were 0.70 ± 0.43 mm, 0.36 ± 0.16 mm, 0.44 ± 0.22 mm, and 0.95 ± 0.43 mm for the superior-inferior (SI), left-right (LR), anterior-posterior (AP), and radial directions, respectively. The overall means ± SDs of the prediction errors were 0.13 ± 0.11 mm, 0.03 ± 0.02 mm, 0.03 ± 0.02 mm, and 0.14 ± 0.11 mm for the SI, LR, AP, and radial directions, respectively. There were no significant differences in these errors between the XLT and 1-View tracking methods. The tumor motion amplitude was moderately associated with the correlation error and strongly related to the prediction error in the SI and radial

directions.

Conclusions: Clinical log data analysis can be used to determine the necessary margin sizes in treatment plans to compensate for correlation and prediction errors in the CyberKnife fiducial-free lung tumor tracking system. The tumor motion amplitude may facilitate margin determination.

Introduction

Stereotactic body radiation therapy (SBRT) is considered a treatment option for stage I non-small-cell lung cancer patients [1, 2]. In SBRT, some techniques for the management of respiratory tumor motion are applied to decrease the irradiated volume of healthy lung tissues [3–6]. Real-time tumor tracking is a technique in which the target location is identified by using a correlation model that incorporates the respiratory movements and the target, which then allows for continuous irradiation that adjusts with respiratory movements [7, 8]. The tracking accuracy depends on the models used in each system [9–11]; therefore, assessment of tracking uncertainties is required to determine the proper margins in treatment plans.

The CyberKnife Synchrony Respiratory Tracking System (Accuray Incorporated, Sunnyvale, CA, US) can perform real-time tracking delivery of SBRT to the lung [5, 7, 12]. The system has 2 orthogonal diagnostic X-ray sources on the ceiling combined with flat-panel detectors under the floor to image the patient's internal targets and correct the beam positions during treatment delivery, thereby minimizing any errors caused by intrafractional patient motion. The respiratory motion of the patient is obtained by a camera array mounted on the ceiling as well as light-emitting diode (LED) markers attached to the patient. For real-time tracking, a correlation model that relates the external LED marker positions to internal target positions is generated before each treatment. The system has also a prediction model that calculates the target's future position to compensate for the mechanical time delay [13, 14]. Currently, 2 real-time tracking methods are available for the CyberKnife Synchrony system: fiducial-based and

fiducial-free tracking methods. Whereas fiducial-based tracking requires fiducial markers implanted near or inside the tumor, fiducial-free tracking allows for direct tumor tracking without the need for implanted fiducials. This avoids the complications associated with the use of fiducial markers such as the risk of pneumothorax, delay of treatment, and irregular tracking owing to fiducial migration and placement. Moreover, the errors caused by interfractional geometry changes, such as those that occur during fiducial-based tracking, can be minimized owing to direct tumor tracking. The fiducial-free tracking algorithm segments a tumor tracking volume (TTV) into small regions and searches the digitally reconstructed radiographs (DRRs) and live radiography images for the intensity pattern most similar to that of the tumor, and thereby localizes the tumor using image registration. There are 2 fiducial-free tracking systems: the Xsight Lung Tracking (XLT) and 1-View tracking systems [15, 16]. The XLT system is available for tumors that can clearly be recognized by 2 X-ray cameras, and tracks the 3-dimensional (3D) position of the target. The 1-View tracking system is used for tumors that are visible on only 1 camera, and tracks each tumor in the plane of motion visible to that camera.

The CyberKnife Synchrony systems generate log files that contain tracking information for each treatment; this allows for the assessment of tracking discrepancies. Previous studies have revealed uncertainties in the correlation and prediction models for fiducial-based tracking by analyzing clinical log data or phantom experiments [13, 14, 17, 18]. However, no studies that closely investigate the accuracy for the fiducial-free tracking systems (XLT and 1-View tracking) have been performed. In contrast to fiducial

markers such as gold spheres, the tracking lung tumor differs in shape, volume, and density per patient; thus, it is unclear if fiducial-free tracking can provide the same tracking accuracy as a fiducial-based tracking system.

In this study, we retrospectively analyzed the Synchrony log files of patients with lung tumors who underwent treatment using the CyberKnife XLT or 1-View tracking system at our institution, and evaluated the clinical correlation and prediction errors. Furthermore, we investigated the tracking tumor-related parameters for these errors.

Methods and materials

Patients

Data from all 42 patients with lung tumors (28 with primary lung cancers and 14 with metastatic tumors) who underwent SBRT using the CyberKnife (VSI, version 9.6.0) XLT or 1-View tracking system without implanted fiducials at our institution between March 2015 and October 2016 were retrospectively analyzed. The patients were treated with a prescription dose of 36–66 Gy in 4–12 fractions depending on each patient's attributes. Before devising a treatment plan, simulations were performed for all patients to determine the tumor tracking method. The XLT system was used for tumors that were clearly visible on 2 X-ray cameras. The 1-View tracking system was used for tumors that were recognizable and tracked with 1 camera but not the other [15]. Visual evaluation to verify that the tumor was tracked correctly by the system was performed by a radiation oncologist and 2 radiation technologists. In case of inadequate tumor visualization with

either camera, patients were considered for implanted fiducials (i.e., for fiducial-based tracking) or for Xsight Spine Tracking (XST; i.e., no respiratory mode tracking); such patients were originally not included in this study. The treatment characteristics are shown in Table 1. The ethics committee of our institution approved this study (reference number: 2017-kenkyu06-02).

CyberKnife treatment plan

The treatment plans were designed on a MultiPlan treatment planning system (version 4.6.0; Accuray Incorporated) using 1.0 mm-thick computed tomography (CT) sections collected from patients with their breaths held at expiration. Data on CT for breath held at inspiration and 4D-CT images were also concurrently obtained. For delineation, the tumor (including the spiculae) as observed under the lung window settings was considered the gross tumor volume (GTV); the clinical target volume (CTV) was equal to the GTV. In the case of 1-View tracking, an internal target volume (ITV) was then generated to account for out-of-plane tumor motion in either camera. The planning target volume (PTV) was derived from the CTV or ITV by adding 3–5 mm margins. Separately, the TTV (which is specifically used for tumor tracking on the CyberKnife fiducial-free tracking system) was delineated based on the identifiable tumor under the mediastinal window settings on primary CT. DRRs were then generated. All the treatment plans were designed using 1 or 2 fixed-size collimators with isocentric or non-isocentric delivery.

Treatment using XLT or 1-View tracking

At the beginning of treatment, the XST System was used to align the patient's translation and rotation based on the skeletal structures by comparing the DRRs. A couch was shifted from the spine alignment center to the center of the motion range of the TTV. Next, a correlation model between the LED markers and TTV positions was constructed based on X-ray images acquired at various respiratory phases. Three types of models were chosen in the system: linear, curvilinear, and dual-curvilinear. The LED marker positions were recorded with a data rate of 28.5 Hz. During treatment delivery, the new X-ray images were acquired at a time interval of approximately 30 s, and the model was continuously updated. Upon beam delivery, the prediction model was used to compensate for the time lag, which was 115 ms in our system. The future tumor position was predicted in advance based on the past pattern of motion [17].

Data analysis for correlation and prediction errors

The following log data files produced by the Synchrony system were obtained after each treatment fraction for each patient: ModelPoint.log, which contains data of the model points and the correlation error; Modeler.log, which contains the output of the correlation model; Predictor.log, which contains the output and error of the prediction model; and ERSIdata.log, which contains the offset values sent to the robot as well as the robot's position [13, 18]. In this study, ModelPoint.log was used to analyze the correlation errors. The data in this file were recorded at the time of each X-ray image acquisition during treatment. The correlation error was defined as the difference between

a tumor's location as determined by X-ray images and that calculated by the latest correlation model. Modeler.log, Predictor.log, and ERSIdata.log were used to analyze the prediction errors. Since these log files were recorded based on robot coordinates, all data were converted into patient coordinates by calculating a 45-degree rotation from the robot coordinates in the inferior and left directions. The prediction error was calculated by comparing the predicted position to the actual position after 115 ms. The overall mean errors of each fraction and the standard deviation (SD) were calculated for each patient for the superior-inferior (SI), left-right (LR), and anterior-posterior (AP) directions. Radial errors were calculated by root-squared summation of each direction.

The impacts of the tracking tumor-related parameters on correlation and prediction errors were investigated by a linear correlation analysis. The tumor-related parameters comprised the tumor motion amplitude, volume, amplitude-to-volume ratio, surface area-to-volume ratio, and density. The tumor motion amplitude in each direction was evaluated from the expiratory and inspiratory phase CT data. The tumor volume, surface area, and density were obtained from the TTV structure on the Velocity software (version 3.2.0; Varian Medical System, Palo Alto, CA, US). The density was defined as the mean CT Hounsfield unit (HU) density of the TTV. The treatment time per fraction and the number of beams were also analyzed.

Statistical analysis

Data are calculated for each patient and expressed as the overall mean ± SD for all patients. The Pearson correlation coefficient r was evaluated with a test of no correlation.

Comparisons were performed using Student's *t*-test, and differences were considered significant at the 95% confidence level ($p < 0.05$). Statistical analyses were conducted using the EZR software (Saitama Medical Center, Jichi Medical University, Saitama, Japan).

Results

Tracking tumor characteristics

As shown in Table 2, the overall mean tumor motion amplitude was 6.7 ± 6.8 mm, 1.4 ± 1.0 mm, 3.5 ± 2.0 mm, and 8.2 ± 6.5 mm in the SI, LR, AP, and radial directions, respectively. The amplitude in the SI direction was significantly larger for lower lobe tumors than for upper or middle lobe tumors (9.0 ± 8.7 mm vs. 4.6 ± 3.3 mm, respectively, $p = 0.03$). The mean tumor tracking volume was 11.7 ± 15.3 cm^3 and the mean tumor density was 26.2 ± 13.8 HU. There were no significant differences on any of the parameters between the XLT and 1-View tracking systems.

Correlation and prediction errors

To assess the model errors from clinical log files, we analyzed the data of 211 fractions from 42 patients. Figures 1 and 2 show histograms of the correlation and prediction errors for all directions, respectively. The mean correlation error was less than 1 mm in the radial direction, whereas the mean prediction errors were very small in all directions. Table 3 summarizes the overall mean correlation and prediction errors. With respect to tumor location, the correlation errors in the SI direction, prediction errors in

the SI direction, and prediction errors in the radial direction were significantly larger for tumors situated in the lower lobes than for upper/middle lobe tumors (0.89 ± 0.52 mm vs. 0.54 ± 0.22 mm, 0.19 ± 0.14 mm vs. 0.08 ± 0.06 mm, and 0.20 ± 0.14 mm vs. 0.10 ± 0.06 mm, respectively; $p < 0.01$).

There were no significant differences in these errors between the XLT and 1-View tracking methods; the correlation errors were 0.93 ± 0.30 mm and 0.96 ± 0.51 mm in the radial direction, respectively ($p = 0.85$). The prediction errors in XLT and 1-View tracking were 0.13 ± 0.08 mm and 0.16 ± 0.14 mm for the radial direction, respectively ($p = 0.42$).

Correlations of tracking tumor-related parameters

The tracking tumor-related parameters were examined to determine their effects on the errors. Table 4 summarizes the regression analysis results. The correlation errors in the SI and radial directions were moderately correlated with the tumor motion amplitude ($r = 0.57$ and $r = 0.55$, respectively; $p < 0.01$). The prediction errors in the SI and radial directions were strongly correlated with the tumor motion amplitude ($r = 0.79$ and $r = 0.79$, respectively; $p < 0.01$). Figures 3 and 4 show the correlation and prediction errors as a function of the tumor motion amplitude in the SI and radial directions, respectively. Other parameters we investigated were not significantly correlated with either the correlation or prediction errors.

Discussion

We successfully described the correlation and prediction errors of the CyberKnife fiducial-free tumor tracking systems via analyzing clinical log files. To our knowledge, no studies have previously investigated clinical model uncertainties in the XLT or 1-View tracking systems; hence, our results ought to provide information regarding proper margins when devising treatment plans for fiducial-free tumor tracking methods. Our data revealed smaller magnitudes of errors than those of previous studies that investigated fiducial-based tracking [13, 14, 17]. For example, Pepin et al. analyzed lung patients using fiducial-based tracking and found that the margin expansions required for 95% coverage of correlation and prediction errors were 2.9 mm and 3.5 mm for the SI direction, respectively [13]. This suggests that the fiducial-free tracking system has different features than those of the fiducial-based tracking system. The positioning of multiple fiducials and the algorithm for detecting the centroid of the fiducial positions on the X-ray images may cause larger errors when using fiducial-based tracking [19, 20]. However, the difference in clinical accuracy between the fiducial-free and fiducial-based tracking methods cannot be estimated definitively, and variations in software versions, patient selection, and analysis methods may also affect the results. While Jung et al. showed that the XLT system had comparable tracking accuracy to that of a fiducial-based system in a phantom study, the clinical settings such as the rigid body errors caused by multiple fiducials were not represented in their study [18].

The tumor motion amplitude was significantly related to both the correlation and prediction errors (Figures 3 and 4). This indicates that a tumor with a large motion amplitude may produce large tracking errors. The same is true for tumor location,

because the tumor motion amplitude was significantly larger for lower lobe tumors than for upper or middle lobe tumors. Portions of our data agree with the findings of Winter et al., who investigated the relationship between fiducial-based tracking errors and motion amplitude in patients with liver cancer [14]; they showed that prediction errors were strongly correlated with target amplitude. In contrast to our findings, however, they also reported that the correlation errors were weakly related to the target amplitude; the differences in tracking methods and tumor sites may explain this discrepancy. Moreover, the results of log data analysis are based on centroid movements of the tumor; however, different areas of the tumor may not move with the same amplitude as the centroid. While the other tumor-related tracking parameters were not correlated with model errors in our study (Table 4), they may still be useful for predicting successful fiducial-free tumor tracking. Bahig et al. reported that the tumor volume and density were the most predictive factors of a successful XLT [21].

There were no differences in errors between XLT and 1-View tracking. This suggests that the 1-View tracking system has comparable tracking accuracy to that of the XLT system, which is noteworthy because the accuracies of these 2 systems have not been previously studied in detail. With respect to the accuracy of fiducial-free tracking algorithms, a study of lung treatment plans by the vendor showed that the 3D root-mean-square tracking error values for XLT and 1-View in-plane tracking algorithms were 1.61 ± 0.64 mm and 1.39 ± 0.63 mm, respectively [15]; the 1-View tracking system appears to have a tracking accuracy that is comparable to that of XLT. However, it should be noted that additional ITV margins are necessary for 1-View tracking to account for the

tumor moving out-of-plane as well as alignment accuracy.

Our study has a few limitations. First, it was difficult to assess the impact of rotations on model errors. Before commencing each delivery, the vertebral structures near the tumor are aligned for translation and rotation directions using the XST system; however, the rotation errors of the tumor are unknown because only a single target is used in the XLT or 1-View tracking system. Another limitation is that the relationships between the model errors and external LED-based motions were not examined. The correlation and prediction models are constructed based on external LED signals; therefore, the respiratory wave motions of the LEDs may affect model errors. However, extracting the specific parameters from the LED marker log data for each patient proved challenging because the CyberKnife treatment duration was long compared to conventional radiotherapy, and each model was continuously updating during the treatment. Additionally, each patient in this study was breathing freely during treatment; hence, some irregular breathing patterns were incorporated into the data. The previous study of liver patients treated with CyberKnife fiducial-based tracking demonstrated that neither the correlation errors nor the prediction errors exhibited a strong correlation with LED marker amplitude and variability [14]. This indicated that the breathing pattern may not be a major factor influencing the tracking accuracy. In contrast, Anetai et al. indicated that the minimum jerk respiratory wave can achieve smooth tracking by CyberKnife [22], and that the specific regular wave motions may be able to reduce tracking errors. Future clinical studies will be required to confirm the impact of breathing patterns on tracking accuracy.

Conclusions

Upon analyzing the correlation and prediction model errors in CyberKnife fiducial-free lung tumor tracking systems using clinical log data, we found that the overall mean correlation error was 0.95 ± 0.43 mm and prediction error was 0.14 ± 0.11 mm in the radial directions. The tumor motion amplitude may be one of the factors that impact these model errors; therefore, the errors should be carefully verified to determine the margins for tumors with large motion amplitudes as accurately as possible. Our results provide critical information in terms of appreciating the error margins when devising treatment plans using CyberKnife fiducial-free tracking methods.

References

1. Chang JY, Senan S, Paul MA, et al. Stereotactic ablative radiotherapy versus lobectomy for operable stage I non-small-cell lung cancer: a pooled analysis of two randomised trials. *Lancet Oncol* 2015;16:630-637.
2. Timmerman R, Paulus R, Galvin J, et al. Stereotactic body radiation therapy for inoperable early stage lung cancer. *JAMA* 2010;303:1070-1076.
3. Rosenzweig KE, Hanley J, Mah D, et al. The deep inspiration breath-hold technique in the treatment of inoperable non-small-cell lung cancer. *Int J Radiat Oncol Biol Phys* 2000;48:81-87.
4. Underberg RW, Lagerwaard FJ, Slotman BJ, et al. Benefit of respiration-gated stereotactic radiotherapy for stage I lung cancer: an analysis of 4DCT datasets. *Int J Radiat Oncol Biol Phys* 2005;62:554-560.

5. Schweikard A, Shiomi H, Adler J. Respiration tracking in radiosurgery. *Med Phys* 2004;31:2738-2741.
6. Keall PJ, Cattell H, Pokhrel D, et al. Geometric accuracy of a real-time target tracking system with dynamic multileaf collimator tracking system. *Int J Radiat Oncol Biol Phys* 2006;65:1579-1584.
7. Ozhasoglu C, Saw CB, Chen H, et al. Synchrony--cyberknife respiratory compensation technology. *Med Dosim* 2008;33:117-123.
8. Kamino Y, Takayama K, Kokubo M, et al. Development of a four-dimensional image-guided radiotherapy system with a gimbaled X-ray head. *Int J Radiat Oncol Biol Phys* 2006;66:271-278.
9. Seppenwoolde Y, Berbeco RI, Nishioka S, et al. Accuracy of tumor motion compensation algorithm from a robotic respiratory tracking system: a simulation study. *Med Phys* 2007;34:2774-2784.
10. Ren Q, Nishioka S, Shirato H, et al. Adaptive prediction of respiratory motion for motion compensation radiotherapy. *Phys Med Biol* 2007;52:6651-6661.
11. Murphy MJ, Pokhrel D. Optimization of an adaptive neural network to predict breathing. *Med Phys* 2009;36:40-47.
12. Nakamura M, Nishimura H, Nakayama M, et al. Dosimetric factors predicting radiation pneumonitis after CyberKnife stereotactic body radiotherapy for peripheral lung cancer. *Br J Radiol* 2016;89:20160560.
13. Pepin EW, Wu H, Zhang Y, et al. Correlation and prediction uncertainties in the cyberknife synchrony respiratory tracking system. *Med Phys* 2011;38:4036-4044.

14. Winter JD, Wong R, Swaminath A, et al. Accuracy of robotic radiosurgical liver treatment throughout the respiratory cycle. *Int J Radiat Oncol Biol Phys* 2015;93:916-924.
15. Accuray, Incorporated. Lung SBRT with the CyberKnife system. White paper provided by Accuray Incorporated. Part number: 500800, Revision: A, 2013. http://www.accuray.com/
16. Bibault JE, Prevost B, Dansin E, et al. Image-guided robotic stereotactic radiation therapy with fiducial-free tumor tracking for lung cancer. *Radiat Oncol* 2012;7:102.
17. Hoogeman M, Prévost JB, Nuyttens J, et al. Clinical accuracy of the respiratory tumor tracking system of the cyberknife: assessment by analysis of log files. *Int J Radiat Oncol Biol Phys* 2009;74:297-303.
18. Jung J, Song SY, Yoon SM, et al. Verification of accuracy of CyberKnife tumor-tracking radiation therapy using patient-specific lung phantoms. *Int J Radiat Oncol Biol Phys* 2015;92:745-753.
19. Xu Q, Hanna G, Grimm J, et al. Quantifying rigid and nonrigid motion of liver tumors during stereotactic body radiation therapy. *Int J Radiat Oncol Biol Phys* 2014;90:94-101.
20. Seppenwoolde Y, Wunderink W, Wunderink-van Veen SR, et al. Treatment precision of image-guided liver SBRT using implanted fiducial markers depends on marker-tumour distance. *Phys Med Biol* 2011;56:5445-5468.
21. Bahig H, Campeau MP, Vu T, et al. Predictive parameters of CyberKnife fiducial-less (XSight Lung) applicability for treatment of early non-small cell lung

cancer: a single-center experience. *Int J Radiat Oncol Biol Phys* 2013;87:583-589.

22. Anetai Y, Sumida I, Takahashi Y, et al. Reference respiratory waveforms by minimum jerk model analysis. *Med Phys* 2015;42:5066-5074.

Table 1. Treatment characteristics.

Characteristics	All plans (*n = 42*)
Tumor location	
Upper or middle lobe	22 (52%)
Lower lobe	20 (48%)
Tracking method	
Xsight Lung	19 (45%)
1-View	23 (55%)
Delivery method	
Isocentric	15 (36%)
Non-isocentric	27 (64%)
Number of fraction	
4 fractions	31 (74%)
8 fractions	7 (17%)
Other	4 (9%)
Mean number of beams (range)	72 (38–118)
Mean treatment time per fraction [min] (range)	27.5 (12.8–51.6)

Table 2. Tracking tumor-related parameters for 42 patients.

Parameters	Mean (range)
Tumor motion amplitude [mm]	
SI	6.7 (0.4–35.4)
LR	1.4 (0.0–3.6)
AP	3.5 (0.4–8.6)
Radial	8.2 (1.9–35.7)
Tumor volume [cm^3]	11.7 (0.5–79.8)
Tumor amplitude/volume [cm^{-2}]	0.3 (0.0–1.6)
Tumor surface area/volume [cm^{-1}]	2.2 (0.8–6.4)
Tumor density [HU]	26.2 (–28.0–44.0)

SI = superior-inferior, LR = left-right, AP = anterior-posterior.

Table 3. Summary of the correlation and prediction errors in 211 fractions.

Error and direction	Mean [mm]	SD [mm]	Range [mm]
Correlation error			
SI	0.70	0.43	0.19–2.51
LR	0.36	0.16	0.13–0.84
AP	0.44	0.22	0.13–1.11
Radial	0.95	0.43	0.39–2.54
Prediction error			
SI	0.13	0.11	0.01–0.45
LR	0.03	0.02	0.01–0.07
AP	0.03	0.02	0.00–0.08
Radial	0.14	0.11	0.02–0.46

SI = superior-inferior, LR = left-right, AP = anterior-posterior.

Table 4. Summary of regression analysis of the correlation and prediction errors.

Parameters	Direction	*r* value	
		Correlation error	Prediction error
Tumor motion amplitude	SI	0.57**	0.79**
	LR	0.14	0.35*
	AP	0.34*	0.37*
	Radial	0.55**	0.79**
Tumor volume	Radial	0.00	0.01
Tumor amplitude/volume	Radial	0.09	0.16
Tumor surface area/volume	Radial	–0.09	–0.12
Tumor density	Radial	0.11	0.01
Number of beams	Radial	–0.12	–0.27
Treatment time per fraction	Radial	0.09	–0.12

SI = superior-inferior, LR = left-right, AP = anterior-posterior, *$p < 0.05$, **$p < 0.01$.

Figure Legend

Figure 1. Distribution of the mean correlation errors in the (a) superior-inferior, (b) left-right, (c) anterior-posterior, and (d) 3-dimensional radial directions in 42 patients.

Figure 2. Distribution of the mean prediction errors in the (a) superior-inferior, (b) left-right, (c) anterior-posterior, and (d) 3-dimensional radial directions in 42 patients.

Figure 3. Correlation errors as a function of tumor motion amplitude for the (a) superior-inferior, and (b) 3-dimensional radial directions.

Figure 4. Prediction errors as a function of the tumor motion amplitude for the (a) superior-inferior, and (b) 3-dimensional radial directions.

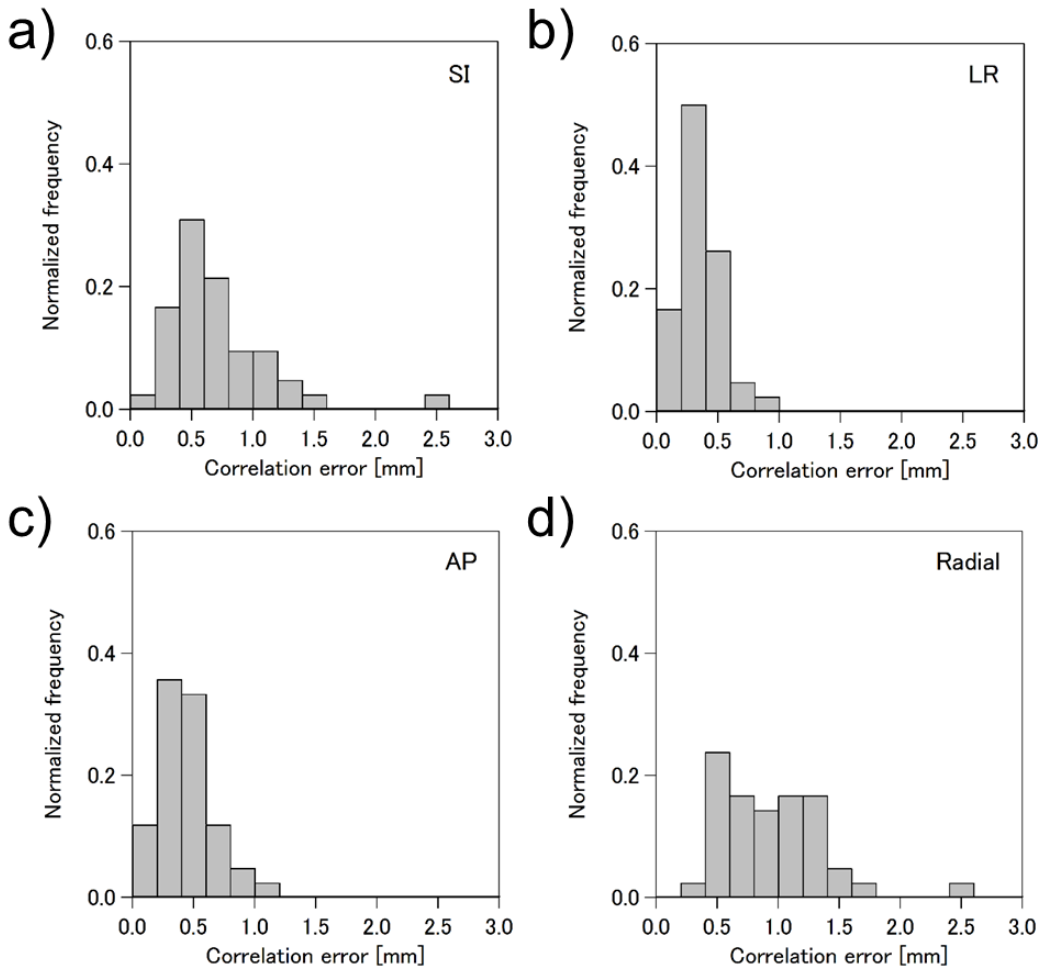
a)
SI
b)
LR
c)
AP
d)
Radial
Normalized frequency
Correlation error [mm]
0.0
0.2
0.4
0.6
0.5
1.0
1.5
2.0
2.5
3.0

Figure 1.

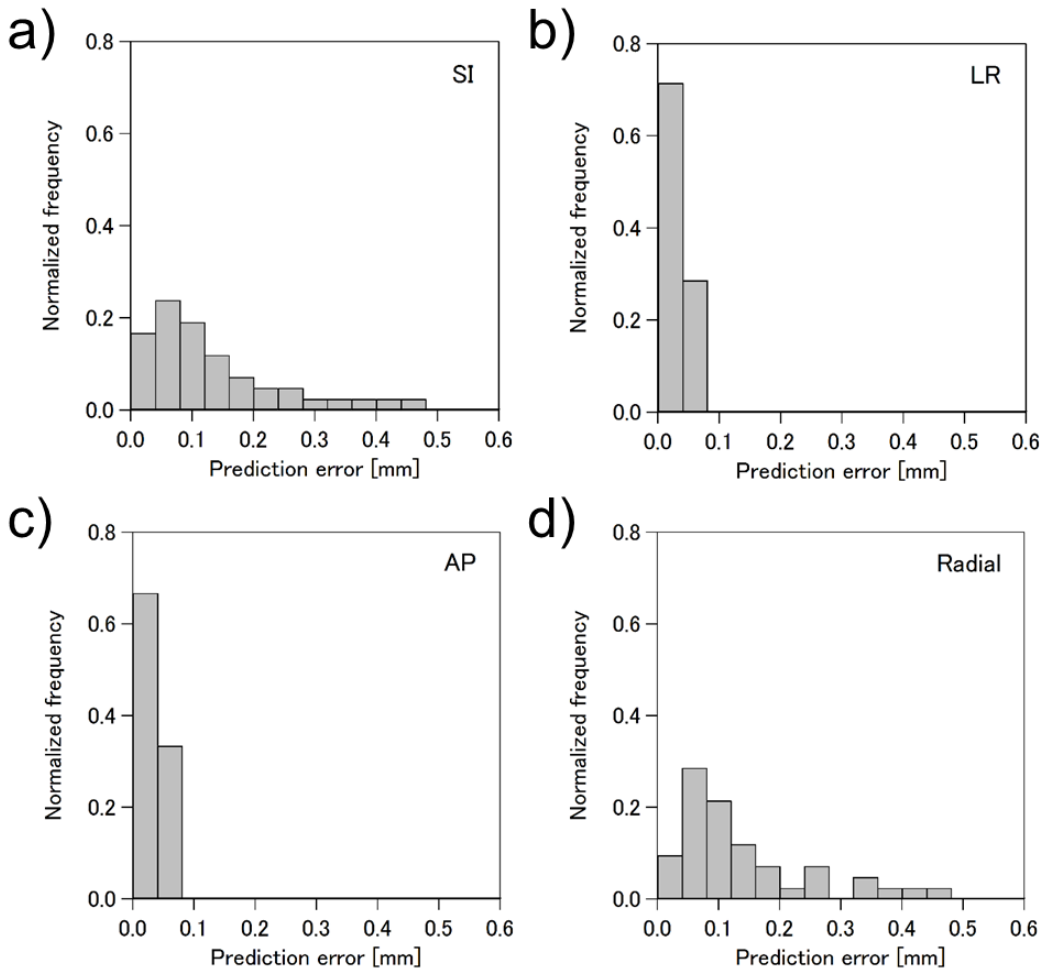
a)
SI
b)
LR
c)
AP
d)
Radial
Normalized frequency
Prediction error [mm]
0.0
0.2
0.4
0.6
0.8
0.1
0.3
0.5

Figure 2.

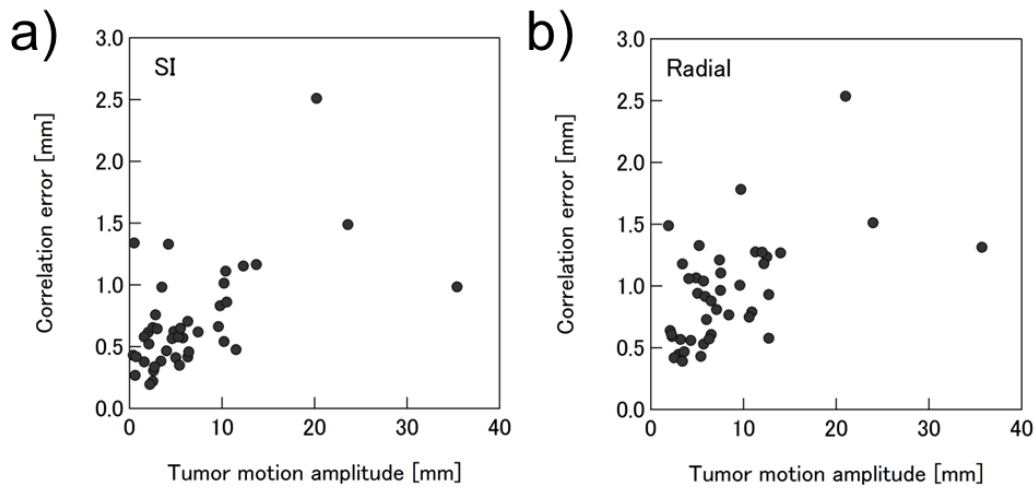
a)
SI
Correlation error [mm]
Tumor motion amplitude [mm]
b)
Radial
Correlation error [mm]
Tumor motion amplitude [mm]

Figure 3.

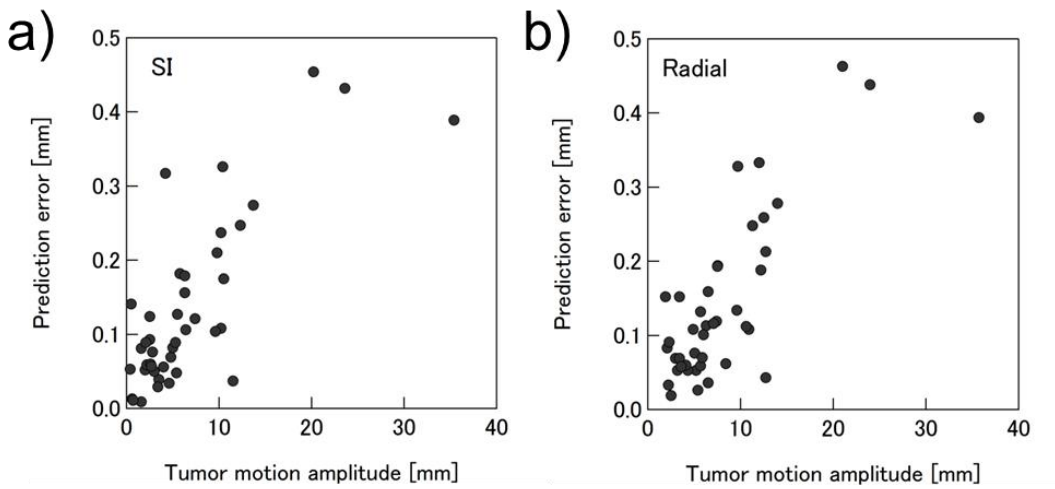
a)
SI
Prediction error [mm]
Tumor motion amplitude [mm]
0.0
0.1
0.2
0.3
0.4
0.5
0
10
20
30
40
b)
Radial
Prediction error [mm]
Tumor motion amplitude [mm]

Figure 4.